

## New regime of small scale density fluctuations in presence of electron heating in Tore Supra

P. Hennequin<sup>1</sup>, L. Vermare<sup>1</sup>, Ö. D. Gürçan<sup>1</sup>, P. Morel<sup>1</sup>, A. Storelli<sup>1</sup>,  
C. Bourdelle<sup>2</sup>, R. Dumont<sup>2</sup> and the Tore Supra team

<sup>1</sup> *Laboratoire de Physique des Plasmas, CNRS, Ecole Polytechnique, 91128 Palaiseau, France*

<sup>2</sup> *CEA, IRFM, F-13108 Saint Paul Lez Durance, France*

Electron heat transport remains a subject of focus of the fusion plasma physics community, in particular because of the residual high level of electron transport through transport barriers while ion thermal and particle transport are quenched [1]. It is suspected that small scale fluctuations [2, 3, 4, 5], less sensitive to ExB shearing, can cause a substantial residual transport, due to the formation of large scale structures (streamers) [6]. Electron heat transport can be produced by large ion scale (ITG/TEM) instabilities, as well as by smaller electron scale (ETG) instabilities, and by the interplay of these scales. Both theoretical and experimental efforts have been drawn to search the evidence of such modes, but their effect on transport remains an open issue [3, 8]

In this paper, we report the observation of a specific high frequency component of density fluctuations at relatively high  $k$  ( $k\rho_s > 1.5$ ), in presence of electron heating (2nd harmonic H heating), that could be related to electron modes, and we analyse the change in turbulence dynamics that accompanies this specific component (long lasting, intense bursts).

### Plasma conditions: dominant electron heating

Tore Supra was operated at reduced field ( $B = 2 - 2.2\text{T}$ ) with ICRH featuring dominant electron heating (2nd harmonic H heating); in this case, the 2H cyclotron layer is close to the magnetic axis, and the production of a fast protons is expected, heating mainly the electrons. The energy content is generally good in these shots (with a better scaling than the usual L mode law), though it depends on the  $n_H/n_D$  fraction: the energy content ( and  $T_e$ ) decreases when H concentration is increased (which is expected to decrease the energy of the fast proton tails). The density was around  $n_e \sim 5 \cdot 10^{19} \text{ m}^{-3}$ ,  $I_p = 0.7 \text{ MA}$ , edge safety factor  $q_a \sim 3.5$ .

### Doppler back-scattering to observe density fluctuations in the medium to high $k$ range

Doppler reflectometry allows a local measurement of density fluctuations at a prescribed perpendicular wave-number; the probing beam is launched in oblique incidence to the cut-off layer, only the back-scattered field is detected. Fluctuations whose wave-number matches the Bragg rule at the cut-off are selected. The signal frequency spectrum is Doppler shifted by  $\Delta\omega = k_{\perp}v_{\perp}$ . The probing beam frequency defines the measurement location; the probing beam incidence selects the wave-number (in the range  $3 < k_{\perp} < 25 \text{ cm}^{-1}$ ). A 3D Gaussian beam tracing code is used to evaluate  $k$  at the cut-off. For the experiments to be discussed here, the X mode W band (75-110 GHz) channel was used, probing  $0.6 < r/a < 0.9$  with  $k$ , in the range

$4 < k < 18 \text{ cm}^{-1}$  ( $1.5 < k\rho_i < 4$ ) [7]. The selected  $\vec{k}_\perp$  can have a small radial component when X mode is used, with  $k_r$  (much) less than  $k_\theta$ , which is ideal for ETG modes that should be streamer-like.

### Additional high frequency component in the Doppler back-scattering signal

As shown in figure 1, a separate small peak appears on the high frequency side of the broad-band frequency spectra measured the Doppler reflectometer, when the beam probes the outer region  $r/a > 0.75$  and for the highest values of the probing wave number [9].

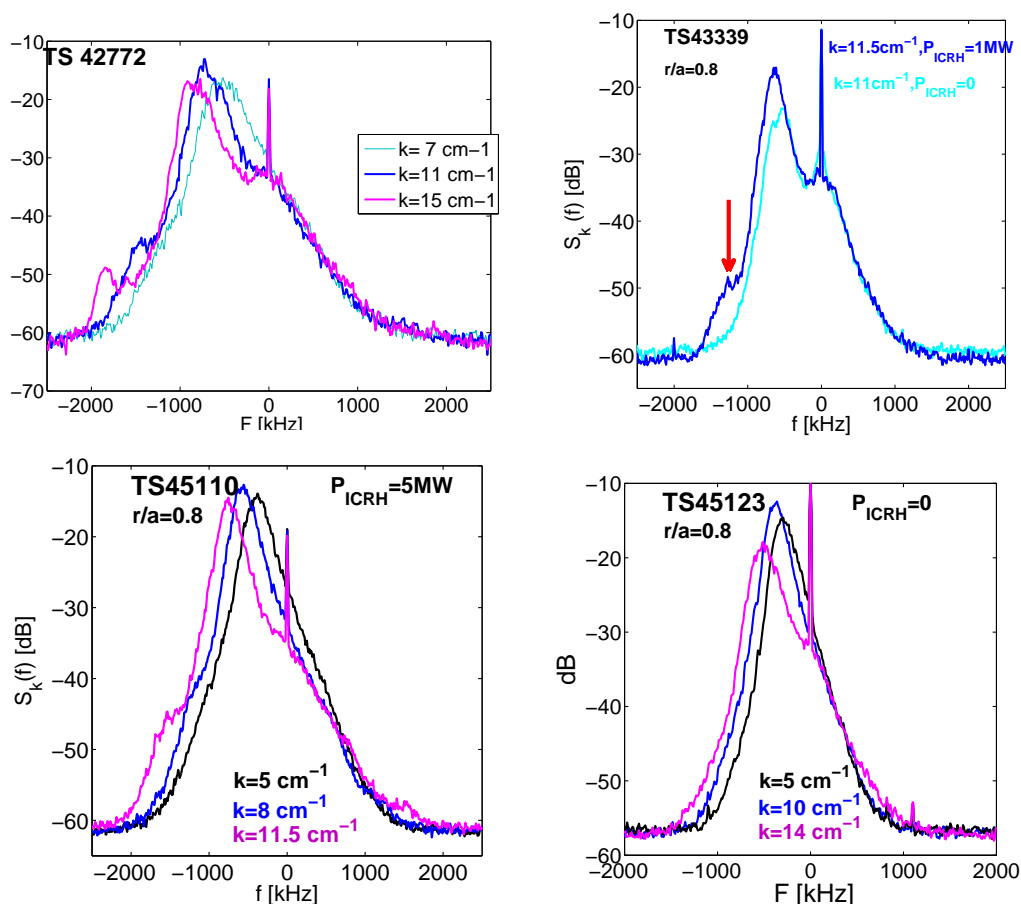


Figure 1: Power spectral density of Doppler back-scattering signals at different probing wave-numbers ( $B = 2.05 \text{ T}$ ): (upper left) ICRH @ 2nd harmonic,  $P = 5 \text{ MW}$ ,  $n_H/n_D < 10$ ; (upper right) with/wo FWEH; (lower left) ICRH 2nd harmonic,  $P = 5 \text{ MW}$  (lower right)  $P = 0$  (Ohmic)

The high frequency component appears also when Fast Wave Electron Heating is used, also expected to heat mainly electrons (Figure 1 upper right). For 2H harmonic ICRH, the strength of the high frequency component is observed to decrease when the  $n_H$  concentration increases, consistently with a lower electron heating effect.

Linear stability analysis (KINEZERO) of these experiments indicates that Electron Temperature Gradient modes are unstable in most of these discharges ( $R/L_{Te} > 15$ ,  $R/L_{Te} > \sim 10$ ,  $RL_n > 6$ ), in the outer region of the plasma ( $r/a > 0.75$ ), and confirmed using the linear gyrokinetic code GENE with the experimental conditions. The maximum frequency of the unstable modes found in the ETG range  $k\rho_i > 2$ , around 600 kHz, is consistent with the experimental value of

the difference  $\Delta f = f_{HF} - f_{LF}$  (frequency difference of the 'electron' and 'ion' components); however this value of  $\Delta\omega = kv_\phi$  is obtained for higher wave number  $k$  than in the experiment. Explaining the high frequency observed in the experiment at the accessible  $k$  should require a higher phase velocity of the mode. This possibility should be checked carefully since other phase velocity measurements in more standard conditions are not well reproduced by the simulations (underestimated) [10].

A spectral doublet is observed similarly on FT2 with high  $k$  UHR measurements [2, 8], sometimes with much higher intensity in the HF component.

### Change in turbulence statistics @ highest $k$

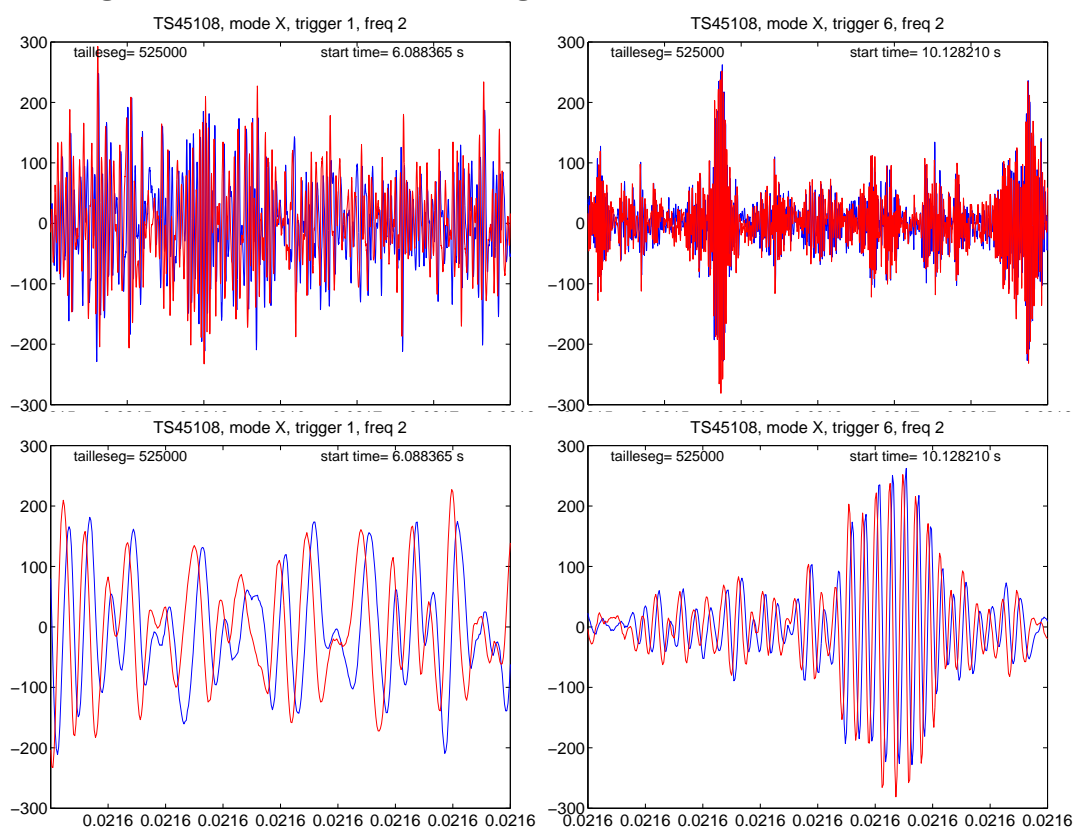


Figure 2: (upper) time series of the raw complex signal (real part in blue, imag in red) at low wave number (left) and high wave number (right), same scales (time and level). (lower) zoom of the upper figure (also same time scales) which shows the different nature of the fluctuations: fast long lasting coherent modes appear at high  $k$ , when the 2nd high frequency peak is present

The presence of this electron component at high  $k$  is accompanied by a change in turbulence dynamics: as seen in the lower right plot of the Figure 2 long lasting bursts of turbulence are observed, a feature which is not seen in usual conditions (left plots). Also the intensity distribution of fluctuation is very different: though the RMS value of the signal is lower at higher  $k$ , these bursts appear with very high intensity (more than 3 times the RMS value), though rarely.

This dynamics change can be quantified by evaluating the signal correlation time and the probability distribution function (PDF) of the fluctuation intensity. PDFs of the signal at low and high  $k$  are plotted in Figure 3, showing wide tails departing from standard PDF (Gaussian functions with same mean and standard deviation as the one of the signals are also plotted (—) and higher values of the kurtosis (4th moment of the signal) at high  $k$ , when the 2nd high frequency peak is present. The turbulence correlation time (Figure 4 left) is much higher when the electron component is observed (at high  $k$ ). It increases with the wave-number, in contrast with the usual  $k$  dependence which is decreasing as  $\tau_c \equiv k^{-1}$ . Similarly, the kurtosis (Figure 4 right) increases with  $k$ .

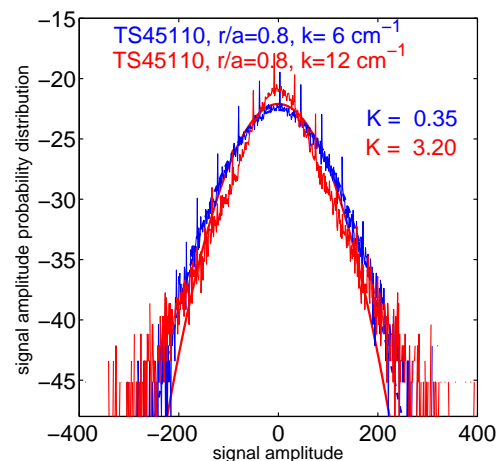


Figure 3: PDF of the back-scattered signal at low (blue) and high (red)  $k$ , with corresponding values of the kurtosis.

These fluctuations are clearly specific, and can be the signature of small scale modes, either unstable in that  $k\rho_i$  range ( 2-3) or in the expected range of ETG ( 8-10) and interacting non linearly with larger ion scales. Also meso-scales (modulational instability) have been predicted to be associated to ETGs [11]. These observations are to be compared to non linear simulations.

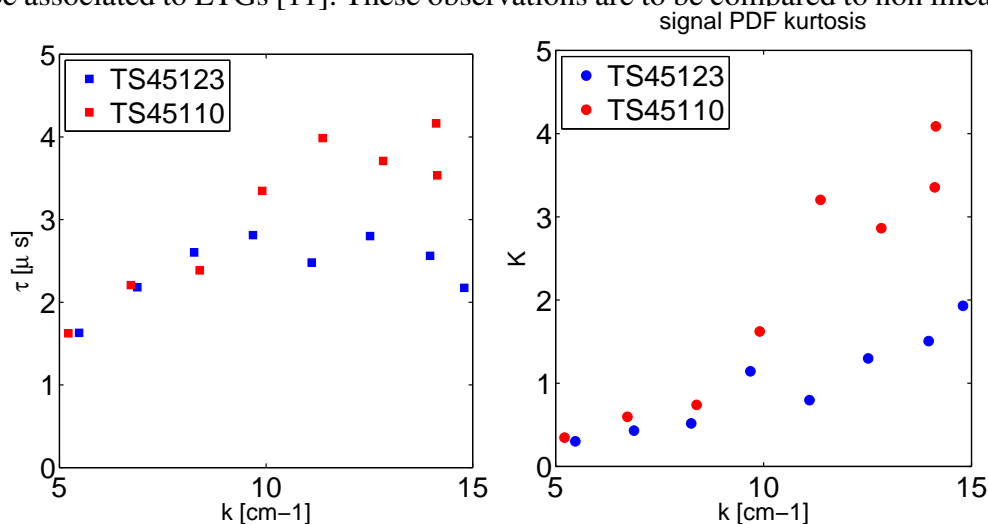


Figure 4: Turbulence correlation time (left) and Kurtosis as a function of the wave number  $k$ .

## References

- [1] B. W. Stallard et al., *Phys Plasmas*, **6**, 1978 (1999)
- [2] E. Gusakov et al., *Plasma Phys. Control. Fusion*, **48** (2006) A371.
- [3] T. Rhodes et al., *Plasma Phys. Control. Fusion*, **49** (2007) B183
- [4] E. Mazzucatto, *Phys. Rev. Lett.*, **101**, 075001 (2008).
- [5] D. Smith, W Guttenfelder et al., *Plasma Phys. Control. Fusion*, **53** (2011) 035013.
- [6] F. Jenko, *Phys. Plasmas*, **7**, 1904 (2000).
- [7] P. Hennequin et al., *Nuc. Fus.* **46**, S771 (2006). L. Vermare et al., *Phys Plasmas* **18**, 012306 (2011).
- [8] A D Gurchenko, E Z Gusakov, et al., *Plasma Phys. Control. Fusion* (2010), 035010.
- [9] P. Hennequin et al., US Transport Task Force Meeting 2009, San Diego.
- [10] L. Vermare et al. 38th EPS Conference on Plasma Physics, Strasbourg, 2011, O4.126
- [11] Ö. Gürçan and P. Diamond. *Phys Plasmas* **11**, 4973 (2005)